Observer Design For RIP Stability Using Takagi-Sugeno Fuzzy Model And Mean Value Theorem

Quy-Thinh Dao, Bao-Trung Dong, and Thi-Van-Anh Nguyen*

School of Electrical and Electronic Engineering, Hanoi University of Science and Technology, Hanoi 100000, Vietnam

Corresponding author. E-mail: anh.nguyenthivan1@hust.edu.vn

Received: Jul. 04, 2024; Accepted: Nov. 05, 2024

This paper presents an observer design for the Rotary Inverted Pendulum (RIP) system using the Takagi-Sugeno (T-S) fuzzy model and the mean value theorem. The proposed method addresses the nonlinear and inherently unstable dynamics of the RIP by transforming the error dynamics into a linear parametric varying system. A non-quadratic Lyapunov function candidate is employed to ensure the global exponential convergence of the estimation error to zero. By combining the differential mean value theorem with sector nonlinearity transformation, the observer guarantees robust performance in the presence of unmeasured premise variables. The stability conditions are derived based on the Lyapunov function, leading to the solvability of a set of linear matrix inequalities. Simulation results demonstrate the effectiveness of the proposed observer in significantly reducing dynamic errors and enhancing the overall stability and accuracy of state estimations. The proposed approach outperforms traditional methods, providing a reliable and precise solution for real-time control applications in nonlinear systems.

Keywords: Observer Design; Takagi-Sugeno Fuzzy Model; Stability control; Mean Value Theorem; Rotary Inverted Pendulum

http://dx.doi.org/10.6180/jase.202509_28(9).0019

1. Introduction

The Takagi-Sugeno (T-S) fuzzy model is a powerful approach for modeling and controlling nonlinear systems [1–6]. It represents complex nonlinear dynamics using a set of local linear models that are blended together through fuzzy membership functions. This framework allows for a systematic formulation of control rules, facilitating the handling of uncertainties and nonlinearities inherent in many real-world systems. The flexibility and robustness of the T-S fuzzy model make it a preferred choice for various control applications.

Observer design based on the T-S fuzzy model has gained significant attention due to its ability to provide accurate state estimations in nonlinear systems [7, 8]. By leveraging the structure of the T-S model, observers can be designed to estimate the internal states of a system from measurable outputs. This is crucial for systems where not all states are directly measurable. The integration of the mean value theorem and sector nonlinearity transformation into observer design enhances the ability to manage nonlinear error dynamics, ensuring stable and reliable state estimation.

This paper proposes an advanced observer design for the Rotary Inverted Pendulum (RIP) system using the T-S fuzzy model and the mean value theorem.

The mean value theorem plays a crucial role in the context of the Takagi-Sugeno (T-S) fuzzy model by enabling the transformation of nonlinear error dynamics into a more manageable form [9, 10]. Specifically, it allows the approximation of the nonlinear behavior of a system by a weighted sum of linear models. In the T-S framework, the mean

value theorem helps in bridging the gap between nonlinear systems and their linear counterparts by ensuring that the nonlinearities are adequately captured and represented through a set of local linear models. This transformation is essential for designing observers and controllers that can handle the inherent complexities of nonlinear systems while maintaining stability and accuracy. By combining the mean value theorem with the T-S fuzzy model, it becomes possible to derive linear matrix inequalities (LMIs) that can be solved to ensure the global exponential convergence of the estimation error, thus enhancing the overall performance and reliability of the control system.

The Rotary Inverted Pendulum (RIP) system is a well-known benchmark for testing control strategies due to its highly nonlinear and inherently unstable dynamics [11, 12]. Effective control of the RIP system is critical for applications in robotics and automation. The proposed T-S fuzzy observer method is applied to the RIP system to validate its performance. The proposed method transforms the nonlinear error dynamics of the RIP into a linear parametric varying system and employs a non-quadratic Lyapunov function candidate to ensure global exponential convergence of the estimation error. By addressing the nonlinearities in the RIP system, the proposed observer enhances the accuracy and stability of state estimations.

The results of the simulation demonstrate the effectiveness of the proposed observer design in significantly reducing dynamic errors and maintaining accurate state estimation over time. The proposed method outperforms traditional approaches, providing a more reliable solution for real-time control applications. The structure of this paper is as follows: Section section 2 details the T-S fuzzy model and the observer design. Section section 3 describes the application of the proposed method to the RIP system. Section section 4 presents the simulation results, and Section section 5 concludes the paper with a summary of the findings.

2. Control design

This section delves into the methodologies employed for designing an effective control system. The focus is on the application of the Takagi-Sugeno (T-S) fuzzy model, which is instrumental in handling the complexities of nonlinear systems. The T-S fuzzy model allows for the systematic formulation of control rules, providing a robust framework for addressing the dynamic behavior of the system. This section also outlines the observer design, which enhances the accuracy of state estimations and improves overall system performance. Additionally, the stability proof of the proposed observer control is provided, ensuring that the estimation error converges asymptotically to zero, thereby guaranteeing the stability of the system.

2.1. T-S fuzzy model

Plant rule i

The Takagi-Sugeno (T-S) fuzzy model is used to represent nonlinear systems through a set of local linear models. These models are combined using fuzzy membership functions to handle system complexities. Each rule in the T-S fuzzy model corresponds to a specific local model.

IF z_1 is θ_{i1}, z_2 is $\theta_{i2}, \ldots, z_p$ is θ_{ip}
THEN

$$\begin{cases} \dot{\mathbf{x}} = A_i\mathbf{x} + B_i\mathbf{u} \\ \mathbf{y} = C\mathbf{x} \quad \text{for } i = 1, 2, \ldots, r \end{cases} \tag{1}$$

Here, $\mathbf{x}$ represents the state vector, $\mathbf{u}$ is the input vector, and $\mathbf{y}$ is the output vector. The matrices A_i and B_i define the dynamics of each local linear model, while C is the output matrix. The index i denotes the rule number, ranging from 1 to r, where r is the total number of rules. The overall system behavior is obtained by blending these local models according to the fuzzy membership functions.

The system (Eq. (1)) can be reformulated as a Takagi-Sugeno fuzzy form:

$$\begin{cases} \dot{\mathbf{x}} = \sum_{i=1}^{r} h_i(\mathbf{z}(\mathbf{x}))(A_i\mathbf{x} + B_i\mathbf{u}) \\ \mathbf{y} = C\mathbf{x} \end{cases} \tag{2}$$

The weighting functions, denoted as $h_i(\mathbf{z})$, are dependent on the premise variables $\mathbf{z}$, where

$$h_i(\mathbf{z}) = \frac{w_i(\mathbf{z})}{\sum_{i=1}^{r} w_i(\mathbf{z})}, \quad w_i(\mathbf{z}) = \prod_{j=1}^{p} M_{ij}^{k}(\mathbf{z}_j). \tag{3}$$

Here, $w_i(\mathbf{z})$ represents the product of the membership functions $M_{ij}^{k}(\mathbf{z}_j)$, each corresponding to the j-th premise variable $\mathbf{z}_j$ in the i-th rule. The summation in the denominator ensures that the weighting functions $h_i(\mathbf{z})$ are normalized, i.e., they sum to 1 across all rules. This normalization is crucial for blending the local models in the Takagi-Sugeno fuzzy system, allowing a smooth transition between different operating regimes based on the values of the premise variables.

2.2. Observer design

This section presents the design of the proposed observer, utilizing the mean value theorem and a non-quadratic Lyapunov function candidate. The observer is designed to improve the accuracy and stability of state estimations in nonlinear systems. The structure and formulation of the observer are thoroughly detailed to ensure clarity and comprehensiveness.

To effectively design the observer for the nonlinear system described in (Eq. (1)), the proposed observer in [13] is structured as follows:

$$\begin{cases} \dot{\hat{\mathbf{x}}} = \sum_{i=1}^{r} h_i(\hat{\mathbf{z}})(A_i\hat{\mathbf{x}} + B_i\mathbf{u}) + \left(\sum_{j=1}^{r_p} h_j(\mathbf{\Lambda})P_j\right)^{-1} L_0(\mathbf{y} - \hat{\mathbf{y}}) \\ \mathbf{y} = C\hat{\mathbf{x}} \end{cases} \tag{4}$$

with $\hat{\mathbf{x}}$ as the estimated state vector, $\hat{\mathbf{y}}$ as the estimated output vector, L_0 as the observer gain, P_j as the observer design matrices, $h_i(\hat{\mathbf{z}})$ as the membership functions (MF) of the system dependent on the estimated states, and $h_j(\mathbf{\Lambda})$ as the membership functions of the observer. The term r_p represents the number of local models or subsystems considered in the observer's structure.

To simplify the formulation of the observer, the following average matrices are introduced:

$$A_0 = \frac{1}{r}\sum_{i=1}^{r} A_i, \quad B_0 = \frac{1}{r}\sum_{i=1}^{r} B_i \tag{5}$$

These matrices represent the averaged dynamics of the system, providing a baseline for further analysis and design.

The Takagi-Sugeno fuzzy system described by Eqs. (2) and (5) can be formulated as

$$\begin{cases} \dot{\mathbf{x}} = A_0\mathbf{x} + B_0\mathbf{u} + \sum_{i=1}^{r} h_i(\mathbf{z})(\overline{A}_i\mathbf{x} + \overline{B}_i\mathbf{u}) \\ \mathbf{y} = C\mathbf{x} \end{cases} \tag{6}$$

with

$$\overline{A}_i = A_i - A_0, \; \overline{B}_i = B_i - B_0.$$

Using Eqs. (4) and (5), the following is obtained:

$$\begin{cases} \dot{\hat{\mathbf{x}}} = A_0\hat{\mathbf{x}} + B_0\mathbf{u} + \\ \quad \sum_{i=1}^{r} h_i(\hat{\mathbf{z}})(\overline{A}_i\hat{\mathbf{x}} + \overline{B}_i\mathbf{u}) + \left(\sum_{j=1}^{r_p} h_j(\mathbf{\Lambda})P_j\right)^{-1} L_0(\mathbf{y} - \hat{\mathbf{y}}) \\ \mathbf{y} = C\hat{\mathbf{x}} \end{cases} \tag{7}$$

The estimation error dynamics, defined as $\mathbf{e} = \mathbf{x} - \hat{\mathbf{x}}$, are described by the following equation:

$$\dot{\mathbf{e}} = \dot{\mathbf{x}} - \dot{\hat{\mathbf{x}}} \tag{8}$$

The goal is to determine the observer gain L_0 that ensures the dynamic estimation error becomes asymptotically stable ($\lim_{t\to\infty} \mathbf{e}(t) = 0$).

Substituting Eqs. (6) and (7) and into Eq. (8) yields:

$$\dot{\mathbf{e}} = \left(A_0 - \left(\sum_{j=1}^{r_p} h_j(\mathbf{\Lambda})P_j\right)^{-1} L_0C\right)\mathbf{e} + \Theta(\mathbf{x}, \hat{\mathbf{x}}, \mathbf{u}) \tag{9}$$

where

$$\Theta(\mathbf{x}, \hat{\mathbf{x}}, \mathbf{u}) = \sum_{i=1}^{r} h_i(\mathbf{z})(\overline{A}_i\mathbf{x} + \overline{B}_i\mathbf{u}) - \sum_{i=1}^{r} h_i(\hat{\mathbf{z}})(\overline{A}_i\hat{\mathbf{x}} + \overline{B}_i\mathbf{u}) \tag{10}$$

Theorem 1 ([14]). Let $D, E \in \mathbb{R}^n$, and let $g(x) : \mathbb{R}^n \to \mathbb{R}^q$ be a differentiable function. There exist vectors $\psi_1, \ldots, \psi_q \in (D, E)$, with the condition that $\psi_i \neq D$ and $\psi_i \neq E$, such that:

For all $i \in I_q$,

$$g(E) - g(D) = \sum_{i=1}^{n}\sum_{j=1}^{n} e_n(i)e_n^T(j)\frac{\partial g_i(\xi)}{\partial x_j}\bigg|_{\psi_i} \times (E - D) \tag{11}$$

Applying Theorem 1, there exists a function $\Psi \in [\mathbf{x}, \hat{\mathbf{x}}]$ such that:

$$\Theta(\mathbf{x}) - \Theta(\hat{\mathbf{x}}) = \sum_{i=1}^{n}\sum_{j=1}^{n} \mathbf{e}_n(i)\mathbf{e}_n^T(j)\frac{\partial \Theta_i}{\partial \mathbf{x}_j}\bigg|_{\Psi_i} \times (\mathbf{x} - \hat{\mathbf{x}}) \tag{12}$$

Consequently, the dynamics of the state estimation error are given by:

$$\dot{\mathbf{e}} = \left(A_0 - \left(\sum_{j=1}^{r_p} h_j(\mathbf{\Lambda})P_j\right)^{-1} L_0C + \sum_{i=1}^{n}\sum_{j=1}^{n} \mathbf{e}_n(i)\mathbf{e}_n^T(j)\frac{\partial \Theta_i}{\partial \mathbf{x}_j}\bigg|_{\Psi_i}\right)\mathbf{e} \tag{13}$$

Assumption. Given that the function $\Theta(\mathbf{x}, \mathbf{u})$ is Lipschitz continuous, its derivatives are bounded, allowing the application of the Sector Non-linearity Transform [15]:

$$\underline{\Theta}_{ij} \leq \Theta_{ij} = \frac{\partial \Theta_i}{\partial \mathbf{x}_j}\bigg|_{\Psi_i} \leq \overline{\Theta}_{ij} \tag{14}$$

where

$$\underline{\Theta}_{ij} = \min\left(\frac{\partial \Theta_i}{\partial \mathbf{x}_j}\bigg|_{\Psi_i}\right) \quad \text{and} \quad \overline{\Theta}_{ij} = \max\left(\frac{\partial \Theta_i}{\partial \mathbf{x}_j}\bigg|_{\Psi_i}\right) \tag{15}$$

The assumption that the function $\Theta(\mathbf{x}, \mathbf{u})$ is Lipschitz continuous plays a critical role in ensuring that its derivatives are bounded. In practical terms, this means that the nonlinear behavior of the system can be confined within a known range. The bounds $\underline{\Theta}_{ij}$ and $\overline{\Theta}_{ij}$ represent the minimum and maximum values of the partial derivative $\frac{\partial \Theta_i}{\partial \mathbf{x}_j}$, respectively, evaluated at the intermediate point Ψ_i. The Sector Non-linearity Transform leverages these bounds to approximate the nonlinearities in a manner suitable for linear analysis. By encapsulating the nonlinear function within these bounds, we can derive linear matrix inequality (LMI) conditions that guarantee stability and convergence in the observer design. This approach allows us to handle the nonlinearities systematically, ensuring that the dynamic estimation error remains stable across a broad operating range.

Any type of nonlinearity can be represented as follows:

$$\Theta_{ij} = \sum_{k=1}^{2} N_{ij}^{k} \sigma_{ijk} \tag{16}$$

where $\sigma_{ij1} = \underline{\Theta}_{ij}$ and $\sigma_{ij2} = \overline{\Theta}_{ij}$

$$\begin{cases} N_{ij}^{1} = \dfrac{\Theta_{ij} - \underline{\Theta}_{ij}}{\overline{\Theta}_{ij} - \underline{\Theta}_{ij}} \\ N_{ij}^{2} = 1 - N_{ij}^{1} \end{cases} \tag{17}$$

$$\sum_{k=1}^{2} N_{ij}^{k}(\Lambda_j) = 1; \quad 0 \le N_{ij}^{k}(\Lambda_j) \le 1 \quad k = 1, 2$$

As a result,

$$\dot{\mathbf{e}} = \left(A_0 - \left(\sum_{j=1}^{r_p} h_j(\mathbf{\Lambda}) P_j \right)^{-1} L_0 C + \sum_{i=1}^{r_p} h_i(\mathbf{\Lambda}) \mathcal{A}_i \right) \mathbf{e} \tag{18}$$

where

$$\sum_{i=1}^{r_p} h_i(\mathbf{\Lambda}) \mathcal{A}_i = \sum_{i=1}^{n} \sum_{j=1}^{n} \mathbf{e}_n(i) \mathbf{e}_n^T(j) \frac{\partial \Theta_i}{\partial \mathbf{x}_j} \bigg|_{\Psi_i} \tag{19}$$

with $r_p \le 2n^2$, and $\mathcal{A}_i$ being dependent on σ_{ijk}.

Ultimately, the dynamics of the state error can be expressed by defining $\Pi_{ij} = \mathcal{A}_i + A_0 - P_j^{-1} L_0 C$.

$$\dot{\mathbf{e}} = \sum_{i=1}^{r_p} \sum_{j=1}^{r_p} h_i(\mathbf{\Lambda}) h_j(\mathbf{\Lambda}) \Pi_{ij} \mathbf{e} \tag{20}$$

2.3. Convergence Condition

This theorem establishes the conditions necessary for ensuring the asymptotic convergence of the state estimation error.

Theorem 2. The state estimation error (Eq. (8)) attains asymptotic stability if there exist positive definite matrices P_i and $Q > 0$ such that the following LMIs are satisfied for $i, j = 1, \ldots, r_p$:

$$P_i > 0 \tag{21}$$

$$(\mathcal{A}_i + A_0)^T P_i + P_i (\mathcal{A}_i + A_0) - C^T L_0^T - L_0 C + (\eta - 1) Q < 0 \quad i = j \tag{22}$$

$$\begin{pmatrix} (\mathcal{A}_i + A_0)^T P_j + P_j (\mathcal{A}_i + A_0) - C^T L_0^T - L_0 C \\ + (\mathcal{A}_j + A_0)^T P_i + P_i (\mathcal{A}_j + A_0) - C^T L_0^T - L_0 C \end{pmatrix} \le 2Q \quad i < j \tag{23}$$

Proof: Choose the Lyapunov function:

$$V(\mathbf{e}) = 2 \int_{\Gamma(0,\mathbf{e})} f^T(\psi) d\psi$$

With $f(\psi) = \sum_{i=1}^{r_p} h_i(\mathbf{\Lambda}) P_i \psi$ and satisfy some property:

- The Lyapunov function is not dependent on the path of the dynamic error.

$$\frac{\partial f_i(\mathbf{e})}{e_j} = \frac{\partial f_j(\mathbf{e})}{e_i} \; \forall i, j = 1 \ldots n \text{ and } f(\psi) = [f_1(\psi),\ f_2(\psi) \ldots f_n(\psi)]$$

- $P_i > 0 \; \forall i = 1 \ldots r_p$.

Choosing $\psi = \alpha \mathbf{e}$ with $\alpha \in \mathbb{R}$, the following is obtained:

$$V(\mathbf{e}) = 2\int_0^1 \alpha \mathbf{e}^T \sum_{i=1}^{r_p} h_i(\mathbf{\Lambda}) P_i \mathbf{e} d\alpha$$

Noting that $2\int_0^1 \alpha d\alpha = 1$, the Lyapunov function can be rewritten as:

$$V(\mathbf{e}) = \mathbf{e}^T \sum_{i=1}^{r_p} h_i(\mathbf{\Lambda}) P_i \mathbf{e}$$

The derivative of the Lyapunov function:

$$\dot{V}(\mathbf{e}) = \dot{\mathbf{e}}^T \sum_{i=1}^{r_p} h_i(\mathbf{\Lambda}) P_i \mathbf{e} + \mathbf{e}^T \sum_{i=1}^{r_p} h_i(\mathbf{\Lambda}) P_i \dot{\mathbf{e}}$$

From the equation (Eq. (9)), the following is obtained:

$$\begin{aligned}\dot{V}(\mathbf{e}) &= \mathbf{e}^T \left(A_0^T P_j - C^T L_0^T + P_j A_0 - L_0 C + \sum_{i=1}^{r_p}\sum_{j=1}^{r_p} h_i(\mathbf{\Lambda}) h_j(\mathbf{\Lambda}) (\mathcal{A}_i^T P_j + P_j \mathcal{A}_i) \right) \mathbf{e} \\ &= \sum_{i=1}^{r_p}\sum_{j=1}^{r_p} h_i(\mathbf{\Lambda}) h_j(\mathbf{\Lambda}) \mathbf{e}^T \left(A_0^T P_j - C^T L_0^T + P_j A_0 - L_0 C + \mathcal{A}_i^T P_j + P_j \mathcal{A}_i \right) \mathbf{e}\end{aligned}$$

According to the Lyapunov theorem, since $\dot{V}(\mathbf{e}) < 0$, the following is obtained:

$$\Omega = \sum_{i=1}^{r_p}\sum_{j=1}^{r_p} h_i(\mathbf{\Lambda}) h_j(\mathbf{\Lambda}) \left(A_0^T P_j - C^T L_0^T + P_j A_0 - L_0 C + \mathcal{A}_i^T P_j + P_j \mathcal{A}_i \right) < 0$$

The result is:

$$\Omega = \sum_{i=1}^{r_p} h_i^2(\mathbf{\Lambda})(\Omega_{ii}) + 2\sum_{i=1}^{r_p}\sum_{i<j}^{r_p} h_i(\mathbf{\Lambda}) h_j(\mathbf{\Lambda}) \left(\frac{\Omega_{ij} + \Omega_{ij}}{2} \right)$$

with $\Omega_{ij} = A_0^T P_j - C^T L_0^T + P_j A_0 - L_0 C + \mathcal{A}_i^T P_j + P_j \mathcal{A}_i$. To $\Omega < 0$, then:

$$\begin{cases} \sum\limits_{i=1}^{r_p} h_i^2(\mathbf{\Lambda})(\Omega_{ii}) < 0 \\ \sum\limits_{i=1}^{r_p}\sum\limits_{i<j}^{r_p} h_i(\mathbf{\Lambda}) h_j(\mathbf{\Lambda}) \left(\dfrac{\Omega_{ij} + \Omega_{ij}}{2} \right) \leq Q \end{cases} \tag{24}$$

As stated in [16]:

$$h_i^2(\mathbf{\Lambda}) - \frac{1}{\eta - 1} \sum_{i=1}^{r_p}\sum_{i<j}^{r_p} 2 h_i(\mathbf{\Lambda}) h_j(\mathbf{\Lambda}) \geq 0$$

with $1 < \eta \leq r_p$. The consequence is:

$$\Omega \leq \sum_{i=1}^{r_p} h_i^2(\mathbf{\Lambda})(\Omega_{ii} + (\eta - 1)Q)$$

The Eq. (24) is hold if only if:

$$\sum_{i=1}^{r_p} h_i^2(\mathbf{\Lambda})(\Omega_{ii} + (\eta - 1)Q) < 0 \tag{25}$$

From Eqs. (24) and (25)), Theorem 2 is derived.

Remark 1: By using the Mean Value Theorem, the unmeasured premise variables in the fuzzy observer are transformed into dynamic errors. This allows for efficient handling of the observer design through LMI conditions.

Remark 2: The approach reduces the conservatism of the LMI conditions through relaxation. Simultaneously, by using the Line Integral Lyapunov function, the observer's performance is improved compared to using the quadratic Lyapunov function. This is demonstrated in the simulation results.

3. Application to rip system

This section demonstrates the application of the T-S fuzzy model to the Rotary Inverted Pendulum (RIP) system. It starts with a detailed overview of the kinematic modeling of the RIP system, then transitions into converting this model into T-S fuzzy equations. Additionally, it discusses the selection of premise variables and the appropriate number of fuzzy rules for the RIP system. The RIP system consists of a servo motor system and two pendulum rods, where the pendulum arm rod has a length denoted by r_a, and the pendulum rod has a length l and a mass m. In this context, θ represents the angle of the pendulum rod with respect to the vertical axis, while ϕ denotes the angle of the pendulum arm with respect to the horizontal axis.

Key parameters of the rotary inverted pendulum system are as follows: The gravitational constant is $g = 9.81\,\mathrm{ms}^{-2}$. The pendulum rod has a mass of $m = 0.125\,\mathrm{kg}$ and a length of $l = 0.335\,\mathrm{m}$. The length of the pendulum arm is $r_a = 0.215\,\mathrm{m}$. The equivalent moment of inertia for the pendulum arm and gears is $J_{eq} = 3.5842 \times 10^{-3}\,\mathrm{kgm}^2$, and the motor rotor's moment of inertia is $J_m = 3.87 \times 10^{-7}\,\mathrm{kgm}^2$. The friction coefficients are $B_a = 0.004\,\mathrm{Nmsrad}^{-1}$ for the pendulum arm and $B_r = 0.0095\,\mathrm{Nmsrad}^{-1}$ for the pendulum rod. The torque constant is $K_t = 7.67 \times 10^{-3}\,\mathrm{NmA}^{-1}$ and the back electromotive force (EMF) constant is $K_v = 7.67 \times 10^{-3}\,\mathrm{Vsrad}^{-1}$. The motor armature resistance is $R = 2.6\,\Omega$. The gearbox ratio is $K_g = 70$, with efficiencies of $\eta_g = 0.9$ for the gearbox and $\eta_m = 0.69$ for the motor.

The state equations for the RIP system can be expressed as

$$\begin{aligned}\ddot{\phi} = {} & 3(s_4 s_5 \sin\phi + s_1 s_4 \sin^3\phi - s_3 s_5 \phi - V_m s_2 s_7 \cos\phi + s_2 s_6 \dot{\theta} - s_2 \dot{\theta}^2 \cos\phi \sin\phi + 2 s_1 s_2 \dot{\phi}\dot{\theta} \cos^2\phi \sin\phi \\ & + s_2 \dot{\theta}^2 \cos\phi \sin^2\phi + s_1 s_5 \dot{\theta}^2 \cos\phi \sin\phi - s_1 s_3 \phi \sin^2\phi)(4 s_1 s_5 - 3 s_2 \cos^2\phi + 4 s_1 \sin^2\phi)^{-1}\end{aligned} \tag{26}$$

$$\begin{aligned}\ddot{\theta} = {} & -(4 s_1 s_6 \dot{\theta} - 3 s_2 s_3 \dot{\phi} \cos\phi - 4 s_1 s_2 \dot{\phi}^2 \sin\phi - 4 V_m s_1 s_7 + 8 s_1 \dot{\phi} \cos\phi \sin\phi + 3 s_1 s_2 \dot{\theta}^2 \cos^2\phi \sin\phi) \\ & (4 s_1 s_5 - 3 s_2 \cos^2\phi + 4 s_1 \sin^2\phi)^{-1} \quad (8)\end{aligned} \tag{27}$$

where the values of $s_1, s_2, s_3, s_4, s_5, s_6, s_7$ are determined by the following formulas:

$$\begin{aligned}& s_1 = \frac{m l r_a^2}{4}, \quad s_2 = \frac{m l r_a}{2}, \quad s_3 = B_r, \quad s_4 = \frac{m g l}{2}, \quad s_5 = J_{eq} + m r_a^2 + \eta_g K_g^2 J_m, \\ & s_6 = B_a + \frac{\eta_m \eta_g K_t K_v K_g^2}{R}, \quad s_7 = \frac{\eta_m \eta_g K_t K_g}{R},\end{aligned} \tag{28}$$

and V_m is the voltage input.

From (Eq. (1)) and $x(t) = [\phi(t)\ \theta(t)\ \dot{\phi}(t)\ \dot{\theta}(t)]^T$, the state equations for the RIP system will be rewritten in T-S form as follows [2]:

$$A = \begin{bmatrix} 0 & 0 & 1 & 0 \\ 0 & 0 & 0 & 1 \\ z_1 z_2 & 0 & z_1 z_3 & z_1 z_5 \\ z_1 z_6 & 0 & z_1 z_7 & z_1 z_8 \end{bmatrix}, B = \begin{bmatrix} 0 \\ 0 \\ z_1 z_4 \\ 4 s_1 s_7 z_1 \end{bmatrix}$$

and

$$\begin{aligned} z_1 &= (4 s_1 s_5 - 3 s_2 \cos^2\phi + 4 s_1 \sin^2\phi)^{-1}, \\ z_2 &= \frac{3 s_4 s_5 \sin\phi + 3 s_1 s_4 \sin^3\phi}{\phi}, \\ z_3 &= -3(s_3 s_5 + s_2 \dot{\phi} \cos\phi \sin\phi), \\ z_4 &= -3 s_2 s_7 \cos\phi, \\ z_5 &= 3(s_2 s_6 \cos\phi + s_2 \dot{\phi}^2 \cos\phi \sin^3\phi + s_1 s_5 \dot{\phi} \sin\phi + 2 s_1 s_2 \dot{\phi} \cos^2\phi \sin\phi), \\ z_6 &= -\frac{3 s_2 s_4 \cos\phi \sin\phi}{\phi}, \\ z_7 &= 3 s_2 s_3 \cos\phi + 4 s_1 s_2 \dot{\phi} \cos^2\phi \sin\phi, \\ z_8 &= -\left(4 s_1 s_6 + 3 s_1 s_2 \dot{\phi} \cos^2\phi + 8 s_1 \dot{\phi} \cos\phi \sin\phi\right). \end{aligned}$$

The Takagi-Sugeno (T-S) fuzzy model is constructed using 256 rules and 8 premise variables. Each rule corresponds to a specific local model that governs the behavior of the system under certain conditions. The premise variables serve as the input conditions for these rules, allowing the model to handle the nonlinear dynamics of the RIP system effectively. This

comprehensive set of rules and variables ensures a detailed and accurate representation of the system's behavior across different operating regimes.

T-S fuzzy observer model for RIP:

$$\dot{\mathbf{e}} = (A_0 - (\sum_{i=1}^{r_p} h_i(\mathbf{\Lambda})P_i)^{-1}L_0C + \mathcal{A})\mathbf{e} \tag{29}$$

We have:

$$\mathcal{A} = \Theta(\mathbf{x}) - \Theta(\hat{\mathbf{x}}) = \begin{bmatrix} \frac{\partial\Theta_1}{\partial\phi}\Big|_{\Psi_{11}} & \frac{\partial\Theta_1}{\partial\theta}\Big|_{\Psi_{12}} & \frac{\partial\Theta_1}{\partial\dot{\phi}}\Big|_{\Psi_{13}} & \frac{\partial\Theta_1}{\partial\dot{\theta}}\Big|_{\Psi_{14}} \\ \frac{\partial\Theta_2}{\partial\phi}\Big|_{\Psi_{21}} & \frac{\partial\Theta_2}{\partial\theta}\Big|_{\Psi_{22}} & \frac{\partial\Theta_2}{\partial\dot{\phi}}\Big|_{\Psi_{23}} & \frac{\partial\Theta_2}{\partial\dot{\theta}}\Big|_{\Psi_{24}} \\ \frac{\partial\Theta_3}{\partial\phi}\Big|_{\Psi_{31}} & \frac{\partial\Theta_3}{\partial\theta}\Big|_{\Psi_{32}} & \frac{\partial\Theta_3}{\partial\dot{\phi}}\Big|_{\Psi_{33}} & \frac{\partial\Theta_3}{\partial\dot{\theta}}\Big|_{\Psi_{34}} \\ \frac{\partial\Theta_4}{\partial\phi}\Big|_{\Psi_{41}} & \frac{\partial\Theta_4}{\partial\theta}\Big|_{\Psi_{42}} & \frac{\partial\Theta_4}{\partial\dot{\phi}}\Big|_{\Psi_{43}} & \frac{\partial\Theta_4}{\partial\dot{\theta}}\Big|_{\Psi_{44}} \end{bmatrix} = \begin{bmatrix} 0 & 0 & 1.0039 & 0 \\ 0 & 0 & 0 & 1.0039 \\ \Lambda_1 & 0 & \Lambda_2 & \Lambda_3 \\ \Lambda_4 & 0 & \Lambda_5 & \Lambda_6 \end{bmatrix}$$

The process involves applying a sector nonlinearity transformation: $\mathcal{A} = \sum_{i=1}^{r^p} h_i(\mathbf{\Lambda})\mathcal{A}_i$ (30)

with $\mathbf{\Lambda} = [\Lambda_1\ \Lambda_2\ \Lambda_3\ \Lambda_4\ \Lambda_5\ \Lambda_6]$, $r_p = 64$.

$$\begin{aligned}
\Lambda_1 &= \{(3s_4s_5cos\phi - 3\dot{\phi}(3\dot{\phi}s_2^2cos^2\phi - 3\dot{\phi}s_2^2sin^2\phi + 6s_1s_3cos\phi sin\phi) - 3\dot{\theta}(3s_2s_6sin\phi + 3\dot{\theta}s_1^2sin^4\phi \\
&\quad - 9\dot{\theta}s_1^2cos^2\phi sin^2\phi - 6\dot{\phi}s_1s_2cos^3\phi - 3\dot{\theta}s_1s_5cos^2\phi + 3\dot{\theta}s_1s_5sin^2\phi + 12\dot{\phi}s_1s_2cos\phi sin^2\phi) \\
&\quad + 9s_1s_4cos\phi sin^2\phi + 9s_2s_7usin\phi)(4s_1s_5 - 3s_2^2cos^2\phi + 4s_1^2sin^2\phi)^{-2} - ((8s_1^2cos\phi sin\phi \\
&\quad + 6s_2^2cos\phi sin\phi)(3\dot{\theta}(3s_2s_6cos\phi + 3\dot{\theta}s_1^2cos\phi sin^3\phi + 3\dot{\theta}s_1s_5cos\phi sin\phi + 6\dot{\phi}s_1s_2cos^{\phi}sin\phi) \\
&\quad - 3\dot{\phi}(3s_3s_5 + 3s_1s_3sin^2\phi + 3\dot{\phi}s_2^2cos\phi sin\phi + 3s_4s_5sin\phi + 3s_1s_4sin^3\phi - 9s_2s_7ucos\phi)))(4s_1s_5 \\
&\quad - 3s_2^2cos^2\phi + 4s_1^2sin^2\phi)^{-2} + 301/2000\}|_{\phi=\Psi_{31}} \\
\Lambda_2 &= -\{(9s_3s_5 + 9s_1s_3sin^2\phi + 18\dot{\phi}s_2^2cos\phi sin\phi - 18\dot{\theta}s_1s_2cos^3\phi sin\phi)(4s_1s_5 - 3s_2^2cos^2\phi + 4s_1^2sin^2\phi)^{-1} \\
&\quad - 101/10000\}|_{\dot{\phi}=\Psi_{33}} \\
\Lambda_3 &= \{(3\dot{\theta}(3s_1^2cos\phi sin^3\phi + 3s_1s_5cos\phi sin\phi) + 9s_2s_6cos\phi + 9\dot{\theta}s_1^2cos\phi sin^3\phi + 9\dot{\theta}s_1s_5cos\phi sin\phi \\
&\quad + 18\dot{\phi}s_1s_2cos^2\phi sin\phi)(4s_1s_5 - 3s_2^2cos^2\phi + 4s_1^2sin^2\phi)^{-1} + 37/10000\}|_{\dot{\theta}=\Psi_{34}} \\
\Lambda_4 &= \{(\dot{\theta}(8\dot{\phi}s_1^2cos^2\phi - 8\dot{\phi}s_1^2sin^2\phi + 3\dot{\theta}s_1s_2cos^3\phi - 6\dot{\theta}s_1s_2cos\phi sin^2\phi) - \dot{\phi}(3s_2s_3sin\phi - 4\dot{\phi}s_1s_2cos\phi \\
&\quad - 3s_2s_4cos^2\phi + 3s_2s_4sin^2\phi))(4s_1s_5 - 3s_2^2cos^2\phi + 4s_1^2sin^2\phi)^{-2} - ((8s_1^2cos\phi sin\phi \\
&\quad + 6s_2^2cos\phi sin\phi)(\dot{\theta}(4s_1s_6 + 8\dot{\phi}s_1^2cos\phi sin\phi + 3\dot{\theta}s_1s_2cos^2\phi sin\phi) + \dot{\phi}(3s_2s_3cos\phi + 4\dot{\phi}s_1s_2sin\phi) \\
&\quad + 4s_1s_7u - 3s_2s_4cos\phi sin\phi))(4s_1s_5 - 3s_2^2cos^2\phi + 4s_1^2sin^2\phi)^{-2} - 153/2500\}|_{\phi=\Psi_{41}} \\
\Lambda_5 &= \{(8s_1^2\dot{\theta}cos\phi sin\phi + 8\dot{\phi}s_1s_2sin\phi + 3s_2s_3cos\phi)(4s_1s_5 - 3s_2^2cos^2\phi + 4s_1^2sin^2\phi)^{-1} - 1/625\}|_{\dot{\phi}=\Psi_{43}} \\
\Lambda_6 &= \{(4s_1s_6 + 8\dot{\phi}s_1^2cos\phi sin\phi + 6\dot{\theta}s_1s_2cos^2\phi sin\phi)(4s_1s_5 - 3s_2^2cos^2\phi + 4s_1^2sin^2\phi)^{-1} - 51/2000\}|_{\dot{\theta}=\Psi_{44}}
\end{aligned}$$

With $\phi \in [-\pi/3; \pi/3]$, $\theta \in [0; 2\pi]$, $\dot{\phi} \in [-5; 5]$, $\dot{\theta} \in [-5; 5]$, $u \in [-10; 100]$, the following table presents the maximum and minimum values of the Λ parameters obtained from the sector nonlinearity transformation:

Table 1. Maximum and Minimum Values of Λ Parameters

Parameter	Λ_1	Λ_2	Λ_3	Λ_4	Λ_5	Λ_6
Max	1717.43	-0.19	12.40	1194.74	2.92	11.32
Min	-1640.92	-5.39	-0.80	-1206.11	-1.33	-5.05

From the model described by 256 rules, the following results are obtained:

$$A_0 = \begin{bmatrix} 0 & 0 & 0.0039 & 0 \\ 0 & 0 & 0 & 0.0039 \\ 0.1505 & 0 & -0.0101 & -0.0016 \\ -0.0612 & 0 & 0.0037 & -0.0255 \end{bmatrix}, B_0 = \begin{bmatrix} 0 \\ 0 \\ -0.0382 \\ 0.0397 \end{bmatrix}$$

From the model described by 256 rules, the following matrices were obtained, which are crucial for the observer design and stability analysis. The state matrices $\mathcal{A}_1$, $\mathcal{A}_8$, $\mathcal{A}_{32}$, and $\mathcal{A}_{64}$ represent different operating conditions of the RIP system, showing variations in system dynamics.

$$\mathcal{A}_1 = \begin{bmatrix} 0 & 0 & 1.0039 & 0 \\ 0 & 0 & 0 & 1.0039 \\ 1717.43 & 0 & -0.186 & 12.40 \\ 1194.74 & 0 & 2.92 & 11.32 \end{bmatrix}, \mathcal{A}_8 = \begin{bmatrix} 0 & 0 & 1.0039 & 0 \\ 0 & 0 & 0 & 1.0039 \\ 1717.43 & 0 & -0.186 & 12.40 \\ -1206.11 & 0 & -1.34 & 5.05 \end{bmatrix}$$

$$\mathcal{A}_{32} = \begin{bmatrix} 0 & 0 & 1.0039 & 0 \\ 0 & 0 & 0 & 1.0039 \\ 1717.43 & 0 & -5.39 & -0.80 \\ -1206.11 & 0 & -1.33 & 5.05 \end{bmatrix}, \mathcal{A}_{64} = \begin{bmatrix} 0 & 0 & 1.0039 & 0 \\ 0 & 0 & 0 & 1.0039 \\ -1640.92 & 0 & -5.39 & -0.80 \\ -1206.11 & 0 & -1.34 & 5.05 \end{bmatrix}$$

The observer gain matrix L_0 and the positive definite matrix Q are designed to ensure the asymptotic stability of the estimation error.

$$L_0 = 10^3 \times \begin{bmatrix} 0.6159 & 0.0495 \\ 0.0493 & 0.413 \\ 8.4539 & -0.0241 \\ -0.0214 & 1.4055 \end{bmatrix}, Q = 10^{-4} \times \begin{bmatrix} 26.547 & -5.564 & -1.029 & -2.300 \\ -5.564 & 21.168 & 1.575 & -0.195 \\ -1.029 & 1.575 & 4.151 & -0.267 \\ -2.300 & -0.195 & -0.267 & 1.116 \end{bmatrix}$$

Additionally, the positive definite matrices P_1, P_8, P_{32}, and P_{64} were determined, which satisfy the required Linear Matrix Inequalities (LMIs) for observer stability.

$$P_1 = \begin{bmatrix} 83135.532 & -177.262 & -4.668 & -2.224 \\ -117.262 & 13989.383 & -1.872 & -6.640 \\ -4.668 & -1.872 & 0.581 & -0.108 \\ -2.224 & -6.640 & -0.108 & 0.070 \end{bmatrix} \times 10^{-4},$$

$$P_8 = \begin{bmatrix} 82910.053 & -193.429 & -4.326 & -0.009 \\ -193.429 & 14005.552 & -0.323 & -6.696 \\ -4.326 & -0.323 & 0.532 & -0.117 \\ -0.009 & -6.696 & -0.117 & 0.068 \end{bmatrix} \times 10^{-4},$$

$$P_{32} = \begin{bmatrix} 82852.839 & -184.488 & -3.414 & 1.087 \\ -184.488 & 14016.899 & -0.076 & -7.712 \\ -3.414 & -0.076 & 0.512 & -0.086 \\ 1.087 & -7.712 & -0.086 & 0.076 \end{bmatrix} \times 10^{-4},$$

$$P_{64} = \begin{bmatrix} 84646.232 & -287.876 & -1.668 & -0.089 \\ -287.876 & 13964.399 & -0.178 & -4.735 \\ -1.688 & -0.178 & 0.508 & -0.519 \\ -0.089 & -4.735 & -0.519 & 0.018 \end{bmatrix} \times 10^{-4}$$

These matrices play a vital role in ensuring that the state estimation error converges to zero, thereby validating the effectiveness of the proposed T-S fuzzy observer model.

However, to ensure stability for the RIP system, the PDC controller designed in [2] is used according to the following diagram:

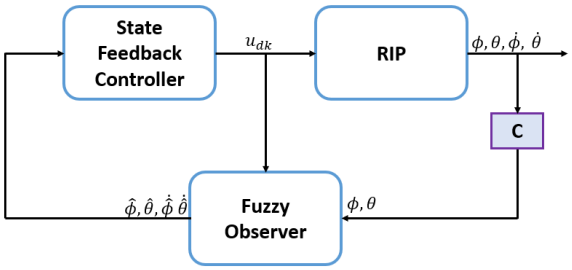

Fig. 1. Control diagram.

The PDC controller requires knowledge of all states of the RIP system, but only information about ϕ and θ is available. Therefore, a fuzzy observer is used to estimate the velocity of the pendulum and the velocity of the pendulum arm.

Algorithm

- Step 1: Design a state feedback controller to stabilize the RIP system.
- Step 2: Design an observer to estimate the unknown states $\dot{\phi}$ and $\dot{\theta}$ of the RIP system.
  - Step 2.1: Formulate the T-S fuzzy model for the RIP system.
  - Step 2.2: Transform the T-S fuzzy model into Eq. (13).
  - Step 2.3: Use the sector nonlinearity transform to derive Eq. (20).
  - Step 2.4: Solve the LMI conditions using MATLAB with YALMIP and MOSEK.
  - Step 2.5: Synthesize the observer using equation (4).
- Step 3: Combine the designed observer and controller to stabilize the RIP system as shown in Fig. 1.

Remark 3: An important assumption in this control design is the applicability of the separation principle, allowing the controller and observer to be designed separately. The proposed observer design can satisfy this principle if it efficiently handles unmeasured premise variables. However, if the system experiences disturbances or noise, this method may not be feasible, as it does not account for these factors during the design process.

4. Simulation results

This section presents the simulation results to validate the performance of the proposed T-S fuzzy observer model for the RIP system. The simulations were conducted to demonstrate the accuracy and stability of the state estimation and to verify the convergence of the estimation error.

To validate our results, a comparison was made with findings from Reference [14], which also utilizes the mean value theorem in its observer design for an induction motor. That study applies a mono-Luenberger observer to a highly coupled system, converting the nonlinear error dynamics into a linear parameter-varying (LPV) system by employing the differential mean value theorem alongside a sector nonlinearity transformation. The stability conditions in that work are derived using a Lyapunov function, leading to the resolution of linear matrix inequalities (LMIs) to ensure global exponential convergence of the estimation error to zero. The simulation results from Reference [14] highlight the effectiveness of their observer design. Similarly, the theoretical principles outlined in Reference [14] are adapted here to design the observer for the RIP system, guaranteeing stability and accuracy in state estimation, as demonstrated inFig. 2.

This figure depicts the dynamic error for the RIP system, showcasing the estimation error in both position and velocity over time. The top subplot illustrates the angular position error (e_ϕ) and (e_θ). The bottom subplot shows the angular velocity error ($e_{\dot{\phi}}$) and ($e_{\dot{\theta}}$). Initially, both the position errors exhibit significant deviations, with the position error reaching approximately -13$\times 10^{-4}$ radians and the velocity error approaching -1 rad/s. However, within the first 0.1 seconds, the observer rapidly corrects these errors, bringing them close to zero. The convergence is smooth and steady, demonstrating the effectiveness of the observer in quickly reducing the dynamic errors. By the end of the 1-second simulation, both errors have nearly stabilized at zero, indicating that the observer accurately estimates both the position and velocity states of the RIP system. This rapid and accurate error correction highlights the robustness and precision of the proposed T-S fuzzy observer model in handling the system's nonlinear dynamics.

Figure 3 shows a detailed analysis of the dynamic error using the proposed T-S fuzzy observer method. The top subplot illustrates the angular position error e_ϕ and e_θ. The bottom subplot shows the angular velocity error $e_{\dot{\phi}}$ and $e_{\dot{\theta}}$. The dynamic errors observed here are significantly smaller than those in Reference [14], which underscores the improved control performance of the proposed method. The error scales in Fig. 3 are in the order of 10^{-6}, demonstrating a finer level of accuracy in state estimation compared to

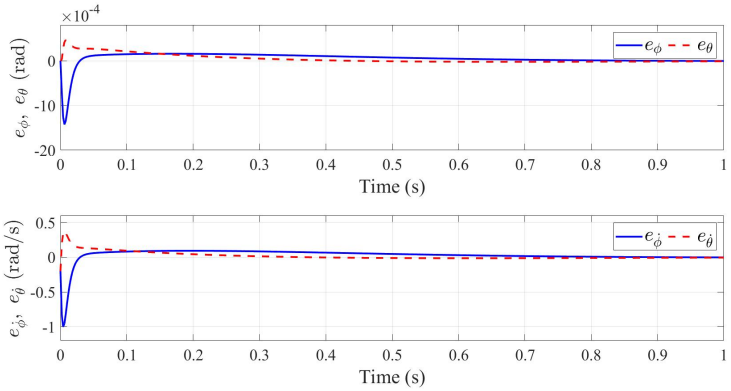

Fig. 2. The dynamic error is using method in [14].

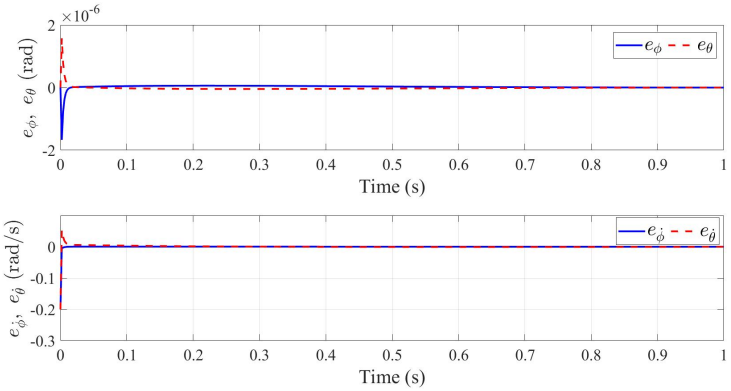

Fig. 3. The dynamic error of proposed method.

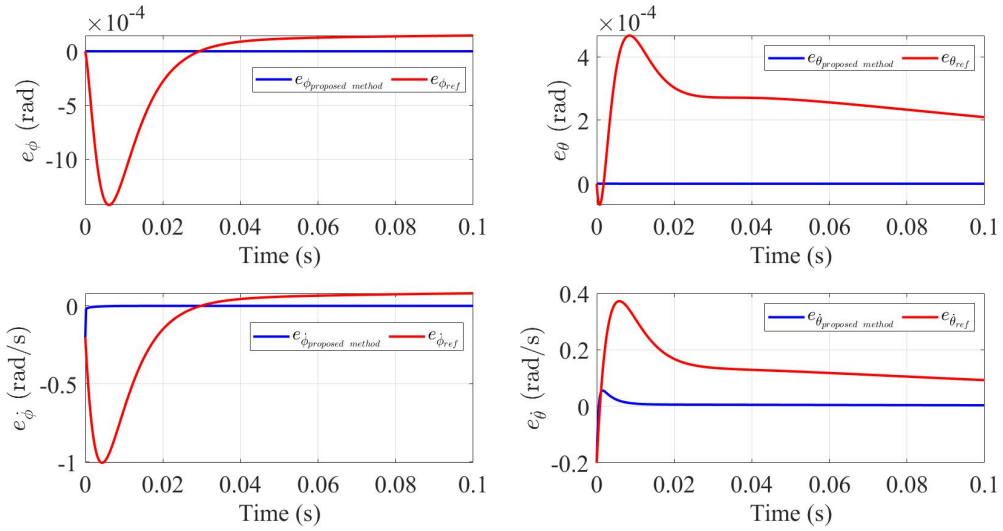

Fig. 4. Dynamic error comparing between the proposed method and method in reference [14].

the reference method. Initially, the errors quickly converge to zero within the first 0.1 seconds, similar to the behavior seen in Fig. 4. However, the magnitude of the errors is much smaller, highlighting the superior precision of the proposed T-S fuzzy observer.

Fig. 5 depicts the estimation of the pendulum and the

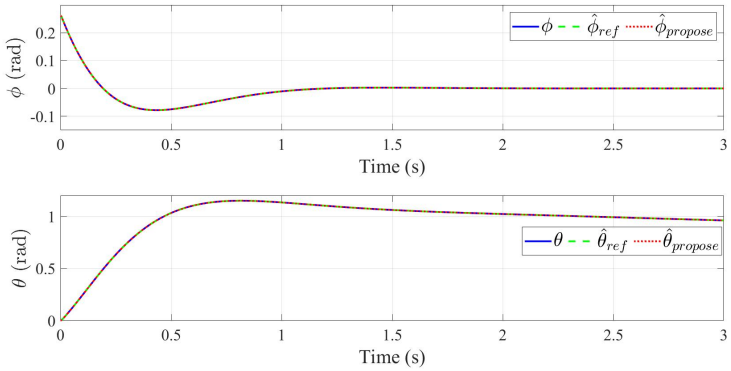

Fig. 5. The estimation of the pendulum and pendulum arm.

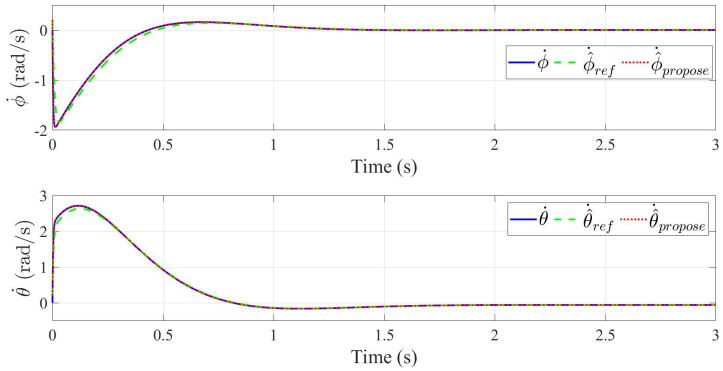

Fig. 6. The estimation of the velocity pendulum and velocity pendulum arm.

pendulum arm. The actual positions of the pendulum and pendulum arm are shown alongside the estimated positions obtained using the T-S fuzzy observer. Initially, there is a slight deviation between the actual and estimated positions, which is quickly corrected by the observer. Within the first 2 seconds, the observer aligns the estimated positions closely with the actual positions, showing minimal error. This close tracking continues throughout the simulation, indicating that the observer can maintain accurate state estimation over time. The figure clearly demonstrates the observer's ability to handle the nonlinear dynamics of the RIP system and the observer's performance in tracking the pendulum and pendulum arm positions underscores its robustness and reliability, providing confidence in its application for control of the RIP system.

Fig. 6 illustrates the estimation of the velocities of the pendulum and the pendulum arm. The actual velocities are plotted alongside the estimated velocities obtained using the T-S fuzzy observer. Initially, there is a notable discrepancy between the actual and estimated velocities, particularly during sudden changes in motion. However, within the first few seconds, the observer adjusts and begins to closely follow the true velocities. Throughout the remainder of the simulation, the estimated velocities remain in close alignment with the actual velocities, demonstrating the observer's capability to accurately estimate the dynamic behavior of both the pendulum and the pendulum arm. The rapid convergence and sustained accuracy in velocity estimation indicate the effectiveness of the observer in managing the nonlinear and dynamic nature of the RIP system. This capability is crucial for precise control applications where accurate velocity information is necessary for feedback and control actions.

Simultaneously, a comparison between the proposed method and the method in reference [14] is conducted to demonstrate the efficiency of the proposed method. As shown in Figures 2 - 6, the performance of the proposed method is better than the approach in reference [14] in terms of both settling time and overshoot of dynamic error.

Overall, the simulation results confirm that the proposed T-S fuzzy observer model enhances the stability and accuracy of state estimation for the RIP system. The ob-

server's ability to handle nonlinearities and uncertainties in the system dynamics is clearly demonstrated, making it a robust solution for control applications.

5. Conclusion

This paper presented an advanced observer design for the RIP system using the T-S fuzzy model and the mean value theorem. By transforming the nonlinear error dynamics into a linear parametric varying system and employing a non-quadratic Lyapunov function candidate, the proposed observer ensures global exponential convergence of the estimation error. Simulation results demonstrated the observer's robustness and precision in reducing dynamic errors and maintaining accurate state estimation over time, significantly outperforming traditional methods. The effectiveness of the T-S fuzzy model in handling nonlinearities and system uncertainties was clearly shown, making the proposed observer a reliable solution for real-time control applications in complex nonlinear systems.

Furthermore, the proposed method is derived based on general theoretical principles, making it extendable to a wide range of nonlinear systems, as long as they meet the necessary assumptions outlined in the observer design. Unlike these prior approaches, the method presented here specifically tackles the stability issue, which enhances its broader applicability. From a theoretical perspective, the proposed method offers an efficient and versatile solution for various nonlinear systems.

Future work will focus on implementing the proposed observer design in real-world scenarios, specifically through experimental validation of physical systems. Additionally, the experimental phase will explore the observer's performance across different nonlinear systems to further confirm its broad applicability.

References

[1] R. Hmidi, A. Ben Brahim, S. Dhahri, F. Ben Hmida, and A. Sellami, (2021) *"Sliding mode fault-tolerant control for Takagi-Sugeno fuzzy systems with local nonlinear models: Application to inverted pendulum and cart system"* **Transactions of the Institute of Measurement and Control** ***43***(4): 975–990. DOI: 10.1177/0142331220949.

[2] T.-V.-A. Nguyen, B.-T. Dong, and N.-T. Bui, (2023) *"Enhancing stability control of inverted pendulum using Takagi–Sugeno fuzzy model with disturbance rejection and input–output constraints"* **Scientific Reports** ***13***(1): 14412. DOI: 10.1038/s41598-023-41258-3.

[3] C.-H. Chiu, Y.-T. Hung, and Y.-F. Peng, (2021) *"Design of a decoupling fuzzy control scheme for omnidirectional inverted pendulum real-world control"* **IEEE Access** ***9***: 26083–26092. DOI: 10.1109/ACCESS.2021.3057658.

[4] C.-C. Ku and S.-H. Jian, (2023) *"Parameter-Dependent Polynomial Fuzzy Control of Nonlinear Inverted Pendulum System"* **International Journal of Fuzzy Systems** ***25***(5): 1770–1781. DOI: 10.1007/s40815-023-01473-6.

[5] M. Rahmawaty, (2021) *"Modeling, Simulation, and Stabilization of a Two-Wheeled Inverted Pendulum Robot Using Hybrid Fuzzy Control"* **Indonesian Journal of electronics, electromedical engineering, and medical informatics** ***3***(3): DOI: 10.35882/ijeeemi.v3i3.2.

[6] M.-L. Nguyen, H.-P. Nguyen, and T.-V.-A. Nguyen, (2024) *"H-Infinity Approach Control On Takagi-Sugeno Fuzzy Model For 2-D Overhead Crane System"* **Journal of Applied Science and Engineering** ***28***: 995–1003. DOI: 10.6180/jase.202505_28(5).0008.

[7] A.-T. Nguyen, V. Campos, T.-M. Guerra, J. Pan, and W. Xie, (2021) *"Takagi–Sugeno fuzzy observer design for nonlinear descriptor systems with unmeasured premise variables and unknown inputs"* **International Journal of Robust and Nonlinear Control** ***31***(17): 8353–8372. DOI: 10.1002/rnc.5453.

[8] M. Ouzaz, A. El Assoudi, et al., (2023) *"Fuzzy Observer Design for State and Fault Estimation for Takagi-Sugeno Implicit Models"* **International Journal of Fuzzy Logic and Intelligent Systems** ***23***(1): 1–10. DOI: 10.5391/IJFIS.2023.23.1.1.

[9] W. Hamdi, M. Y. Hammoudi, and A. Boukhlouf, (2023) *"Observer Design for Takagi–Sugeno Fuzzy Systems with Unmeasurable Premise Variables Based on Differential Mean Value Theorem"* **Engineering Proceedings** ***58***(1): 28. DOI: 10.3390/ecsa-10-16008.

[10] K. Mimoune, M. Y. Hammoudi, R. Saadi, M. Benbouzid, and A. Boukhlouf, (2023) *"Real-time implementation of non linear observer based state feedback controller for induction motor using mean value theorem"* **Journal of Electrical Engineering & Technology** ***18***(1): 615–628. DOI: 10.1007/s42835-022-01274-1.

[11] Y. Kim, Y. Lee, S. Lee, and O. Kwon. "T-S fuzzy controller design for Rotary Inverted Pendulum with input delay using Wirtinger-based integral inequality". In: *2022 22nd International Conference on Control, Automation and Systems (ICCAS)*. IEEE. 2022, 890–895. DOI: 10.23919/ICCAS55662.2022.10003811.

[12] D.-B. Pham, Q.-T. Dao, N.-T. Bui, and T.-V.-A. Nguyen, (2024) *"Robust-optimal control of rotary inverted pendulum control through fuzzy descriptor-based techniques"* **Scientific Reports *14***(1): 5593. DOI: 10.1038/s41598-024-56202-2.

[13] K. Mimoune, M. Hammoudi, W. Hamdi, and S. Mimoune, (2023) *"Observer design for Takagi–Sugeno fuzzy systems with unmeasured premise variables: Conservatism reduction using line integral Lyapunov function"* **ISA transactions *142***: 626–634. DOI: 10.1016/j.isatra.2023.07.039.

[14] M. Y. Hammoudi, A. Allag, M. Becherif, M. Benbouzid, and H. Alloui, (2014) *"Observer design for induction motor: an approach based on the mean value theorem"* **Frontiers in Energy *8***: 426–433. DOI: 10.1007/s11708-014-0314-x.

[15] D. Ichalal, B. Marx, S. Mammar, D. Maquin, and J. Ragot. "Observer for Lipschitz nonlinear systems: Mean Value Theorem and sector nonlinearity transformation". In: *2012 IEEE International Symposium on Intelligent Control*. 2012, 264–269. DOI: 10.1109/ISIC.2012.6398269.

[16] B.-J. Rhee and S. Won, (2006) *"A new fuzzy Lyapunov function approach for a Takagi–Sugeno fuzzy control system design"* **Fuzzy sets and systems *157***(9): 1211–1228. DOI: 10.1016/j.fss.2005.12.020.